Article, Author's Postprint

Ulm, Marius; Niehüser, Sebastian; Kondziella, Bernhard; Arns, Arne; Jensen, Jürgen; Uliczka, Klemens

Field Measurements in the Kiel Canal, Germany: Ship Waves, Drawdown, and Sediment Transport

Journal of Waterway, Port, Coastal, and Ocean Engineering

Erstveröffentlichung in Journal of Waterway, Port, Coastal, and Ocean Engineering 4(2020). Verfügbar unter https://doi.org/10.1061/(ASCE)WW.1943-5460.0000577

Field Measurements in the Kiel Canal, Germany: Ship Waves, Drawdown, and Sediment Transport

Marius Ulm[a], Sebastian Niehüser[a], Bernhard Kondziella[b], Arne Arns[a], Jürgen Jensen[a], Klemens Uliczka[b]

[a] University. of Siegen, Research Institute for Water and Environment

[b] Federal Waterways Engineering and Research Institute, Dep. Hydraulic Engineering in Coastal Areas, Hamburg, Germany

Abstract: Ship waves and ship-induced flows are the main hydrodynamic loads on waterway beds and embankments. However, the underlying physical processes are not yet understood fully. Recent field measurements, conducted in the Kiel Canal, Germany, allow a better understanding of these loads and the resulting (ship-induced) sediment transport. The measurements include high-resolution time series of pressure, three-dimensional flow velocities, and turbidity, collected using stationary as well as vessel-mounted sensors. The focus of this paper is on two aspects. First, existing drawdown estimation approaches are reviewed and validated against field measurements. Based on this, a new approach is derived to improve the general description of ship waves in confined waters. Second, a new approach to estimate the ship-induced sediment transport in the Kiel Canal is developed using turbidity and flow measurements and validated against dredging volumes. Our results show that about 10% of the total transported sediment volume in the Kiel Canal can be attributed to ship traffic, whereas the remaining volume is mainly transported during regular dewatering periods. This paper provides an empirical-based method to estimate ship-induced sediment transport in artificial waterways as basis for future canal management strategies. DOI: 10.1061/(ASCE)WW.1943-5460.0000577. © 2020 American Society of Civil Engineers.

Note: This manuscript was submitted on September 14, 2019; approved on January 6, 2020; published online on April 28, 2020. Discussion period open until September 28, 2020; separate discussions must be submitted for individual papers. This paper is part of the Journal of Waterway, Port, Coastal, and Ocean Engineering, © ASCE, ISSN 0733-950X.

Introduction

The maintenance of waterways is an enduring and expensive task for federal authorities. Running costs are incurred because of the permanent dredging and disposing of accumulated sediments as well as repair and reinforcement of bank revetments. Each year more than 40×10^6 m^3 have to be dredged from German coastal waterways to maintain safe ship navigation and port operation (Weilbeer 2014), with costs of several million Euros. Up to 20 % of the total dredging volume arises from the Kiel Canal alone (Brockmann et al. 2008), one of the world's busiest artificial waterways. Lowering running dredging and maintenance costs can mainly be achieved in two ways. First, ship-induced loads on waterways need to be reduced. Here, ship-induced loads are defined as the hydrodynamic effects resulting from a passing vessel including water level depression, flow velocities, and ship waves. For example, Rapaglia et al. (2015) proposed stricter speed limits for vessels in the Venice Lagoon, Italy, to reduce ship-induced loads on the waterway beds in the lagoon. Pesce et al. (2018) used these findings as one component within their analysis of alternative navigation routes. Second, running costs could also be lowered by enhancing current waterway design approaches, but therefore detailed knowledge of the underlying processes is required. Ship-induced loads appear to have a determining influence on future ship traffic management. To meet these challenges, the German Federal Waterways Engineering and Research Institute (BAW) started a joint research project including a field campaign to answer these open research questions to (i) quantify the ship-induced loads on waterways and to (ii) derive management recommendations for responsible authorities. Specifically, the drawdown and the ship-induced amount of the total transported sediments are addressed within this study. A challenge of future ship traffic management will be the minimization of the impact of individual vessels on waterways, for which a quantification of the ship-induced loads is essential. The described investigations summarize the main results of the research project based on the field measurements.

The first laboratory and field experiments of the BAW on ship-waterway interaction date back to the 1990s showing that ship-induced flows and pressure changes lead to resuspension and transport of bed sediments (Flügge Uliczka 1996). As physical transport processes and the impact of passing ships on these processes had not yet been explored fully, the need for further research in the field of ship-induced sediment transport was then pointed out, e.g., by Flügge Uliczka (1996). A key challenge is the separation of vessel-resuspended sediment from the total amount of sediment within the water column. Measuring vessel loads under laboratory-like conditions are required for distinguishing between these components, because natural influences such as tidal or discharge currents can be neglected. The Kiel Canal provides these laboratory-like conditions because both ends of the canal are closed by locks and dewatering currents occur only at specific times.

In 2012, the BAW conducted a field campaign to assess the aforementioned research questions for the Kiel Canal by recording hydrodynamic loads as well as sedimentological parameters of about 500 vessel passages (Uliczka Kondziella 2016). Similar field campaigns have revealed the importance of a detailed assessment of waterway morphology. Zaggia et al. (2017) highlighted that heavy ship traffic is the main driver of shoreline changes at the Malamocco Marghera Channel in the Venice Lagoon. Vessel-induced drawdown flows led to an estimated total sediment loss of 1.19×10^6 m^3 within 47 years in this area. The relationship between drawdown and sediment resuspension was also described by Göransson et al. (2014), who investigated ship-induced loads on bed and banks of the Göta Älv waterway in Sweden. Houser (2011) also used field measurements and focused on ship waves and associated sediment transport in the estuarine Savannah River, USA. Houser (2011) highlighted differences between subcritical and supercritical cruise and showed the impact of turbulent flow velocities expressed as turbulent kinetic energy. Houser (2011) concluded that there is a strong dependency between an increasing turbulent kinetic energy leading to an accelerated sediment resuspension.

The ship-induced hydrodynamic loads on waterways are primarily caused by the movement of a vessel relative to the movement of the surrounding water body. In shallow and confined waters such as harbors, propeller wash is also one of the most important loads, as described, e.g., by Hamill et al. (1999). The presented research focuses on large waterways, where propeller wash can be neglected owing to a sufficient under-keel clearance and a constant vessel speed. Hence, it is essential to improve the understanding of ship wave generation as the main hydrodynamic load. In general, ship waves are separated into a primary wave system, which is characterized by a remarkable water level depression called drawdown with long periods, and a secondary wave system with shorter periods. The drawdown occurs due to the ship's water displacement and consequently the ship reduces the canal cross section. As the volumetric flow rate is constant, flow velocity increases in the area where the displacement reduces the canal cross section. Following Bernoulli's principle, the water surface elevation is reduced in these areas with increased flow velocities. The so-called return flow between ship and canal bed may exceed sediment-dependent critical flow velocities resulting in a resuspension and transport of bed material. The wave systems additionally affect the waterway banks. Fig. 1(a) shows the resulting characteristic wave pattern of a vessel in displacement mode. Fig. 1(b) shows corresponding dimensions that either describe the wave pattern (e.g., drawdown z_S, bow wave s_B, stern wave H_s), or have a direct influence on the wave heights (e.g., relative vessel speed v_{rs} and the aforementioned ship cross section A_S and canal cross section A). The blocking coefficient n combines ship and waterway parameters to account for the interaction between the vessel and the characteristics of the observed cross section. The coefficient is defined as the canal cross section divided by the ship cross section at the considered location. Furthermore, the distance between sailing line and bank determines whether the primary or the secondary wave system causes higher impacts on the bank.

Theoretical approaches for the estimation of ship wave heights are based on fundamental principles of hydraulics: conservation of mass, energy, and momentum. The application of the consequential laws (i.e., continuity law, Bernoulli's law) requires model assumptions such as a stable return current and negligibleness of secondary waves, friction losses, and vessel dynamics such as yaw, pitch, and roll movement. Several published studies developed approaches for the estimation of ship-induced wave heights, generally described using the drawdown z_S, but building on different assumptions and boundary conditions. Commonly used approaches were developed by Krey (1913), Constantine (1960), Bouwmeester et al. (1977), Gelencser (1977), Dand White (1977), Führböter et al. (1984), and PIANC (1987). All the equations describe, in simplified terms, the drawdown z_S with a function of waterway geometry, vessel geometry, and vessel movement (Jensen 1998). The mathematical descriptions of the drawdown z_S can be based on purely analytically determined approaches or existing physical relationships. Often a combination of both is used. As these approaches are all adjusted to

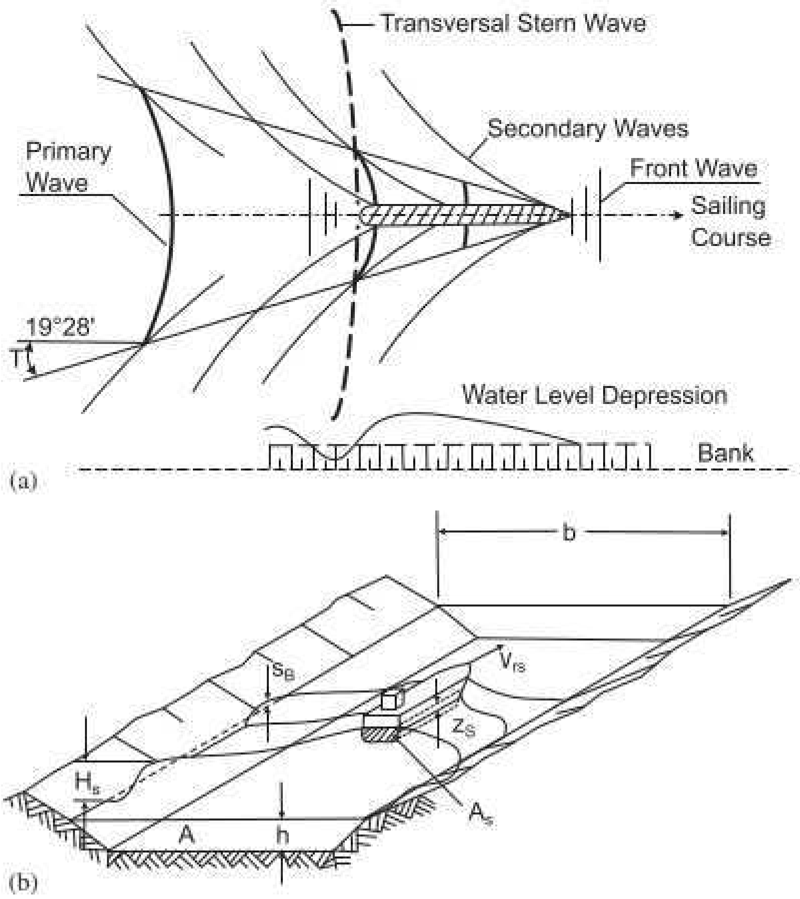

Figure 1: Explanation of the primary and secondary ship wave system (a) and ship-induced water motion in channels (b)

specific conditions by including empirical parameters, the results show large differences when calculating the drawdown with each approach using the same database, as shown within the discussion. The aforementioned simplifications include but are not limited to neglecting friction effects or assuming homogeneous cross sections, which both affect the results and the associated uncertainties. The existing empirical approaches have been developed for specific engineering or research issues and mostly rely on less input data. To overcome these limitations and to reduce the uncertainties, Rapaglia et al. (2011) and Gelinas et al. (2013) evaluated field measurements in the Venice Lagoon based on a regression approach of Schoellhamer (1996) and were able to explain 81% of the variability of the drawdown. Based on their findings, Rapaglia et al. (2011) concluded that ship speed is more important regarding the drawdown than the ship size. Furthermore, the regression approach of Schoellhamer (1996) has also been derived and adjusted to the dataset in an earlier state of the presented research project and is actually replaced by the newly developed drawdown estimation approach, as described in this paper. The present dataset of field measurements allows a derivation of an approach completely based on physical laws and represents an added value (see the section “Drawdown Estimation”).

Previous studies have also focused on numerical simulations to describe ship-induced waves and flows in waterways (e.g., Dam et al. 2008; Gharbi et al. 2010; Ji et al. 2014). However, such numerical models are generally restricted by the underlying boundary conditions such as the ship's hull geometry or inlet/outlet conditions as well as simplified canal geometries. The results help to describe flows in detail, but still lack the unknown processes contained in the data from field measurements.

Study Area

The Kiel Canal has a total length of 98.64 km connecting Brunsbüttel at the tidal Elbe River with Kiel at the Baltic Sea [see Fig. 2(a)] (e.g., Brockmann et al. 2008; Thormählen 2010). In 2012 about 35,000 vessels travelled through the Kiel Canal. Using the Kiel Canal reduces the route between the North Sea and the Baltic Sea by several hundreds of kilometers because the ships can avoid travelling around northern Denmark. This highlights the crucial role of the Kiel Canal for regional economics as well as for the trans-European infrastructure. The distance and time benefits generate a great economic advantage for international shipping. The shortcut also leads to a reduction of CO_2 emissions owing to fuel savings (Brockmann et al. 2008). The Kiel Canal has a trapezoidal cross section with a waterline width of approximately 160 m after the last widening in 1966. Only the last 20 km of Kiel are still limited to about 100 m. Two-way traffic and overtaking of large ships is limited to wider passing places in this canal section. The bottom width of 90 m and the mean water depth of 12 m lead to a slope angle of about 1:3. The attached embankment has a flat slope and is designed to withstand wave impacts, water level depression, and return currents due to the passing vessels (IKC 2013). The locks at both ends of the Kiel Canal and the homogeneous cross section lead to constant and stationary conditions, for example with regard to the flow velocities, which only reach a magnitude of approximately 0.15 m/s during dewatering periods. The sediments at the measurement site are mainly composed of very fine sand (19%), fine sand (38.4%), and medium sand (17.6%). This composition covers the principal grain fractions in German coastal waterways, so that results are mostly transferable. The following investigations focus on these three main grain diameters, which yield a cumulated mass fraction of 75%. The grain fractions were determined by using four soil samples, taken only during the measurements (Aqua Vision BV, Suspended sediment measurements in the Nord-Ostsee-Kanal, unpublished report). Therefore, no reliable measurements regarding the spatial and temporal development are available. However, because there is no significant sediment input from outside the Kiel Canal (e.g., dumping of dredged material or larger inflows), it can be assumed that the sediment composition at the bottom only changes marginally. Furthermore, the Kiel Canal is regularly kept maintained by dredging and, hence, should be quasi-stationary in time. Owing to the length of the canal and the different landscape types, it is reasonable that there are also different sediment compositions in other canal sections that are, however, not relevant for the intended investigations based on a specific cross section.

In general, the traffic in restricted waterways shows an increase of larger and faster ships that generate surface waves and currents that have the potential to cause serious damage to embankments and seawalls (e.g., Bezuijen Köhler 1996; Jensen 1998). The development of the traffic, especially in the Kiel Canal, can be described based on two field campaigns performed by BAW in 1998 and 2012. The latter will be introduced and analyzed subsequently. Vessels passing through the Kiel Canal are classified by traffic classes depending on the ship's geometry. The higher the class number, the larger

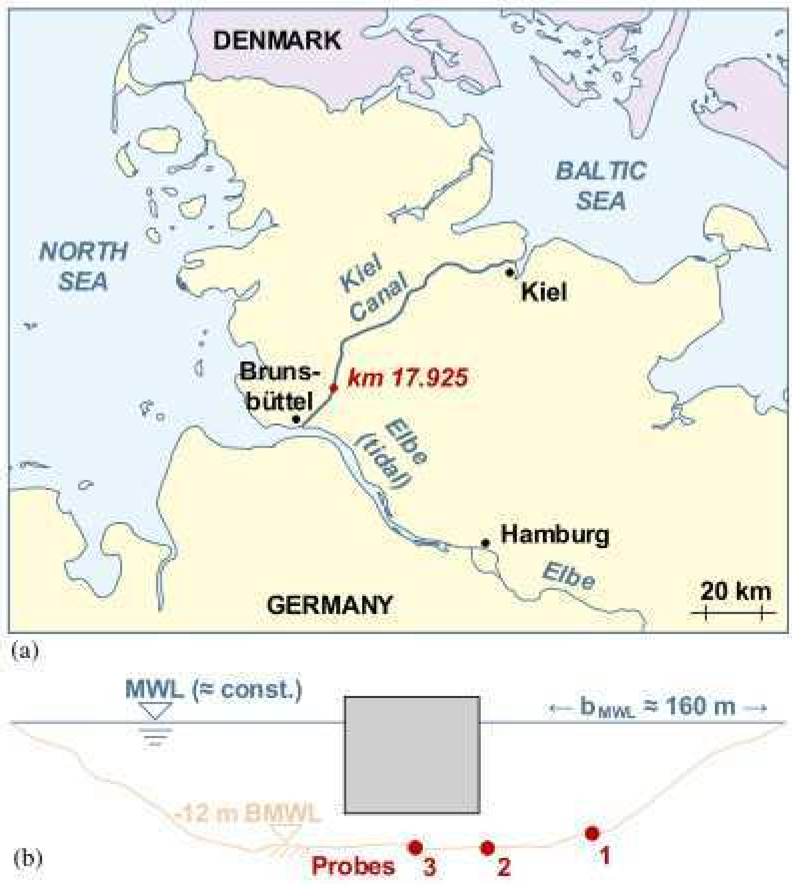

Figure 2: (a) Map of the study area with the field campaign location at km 17.925; and (b) cross section at the field measurement location with probe locations and an example vessel geometry (gray box). (Adapted from Ulm 2017)

the vessel. The comparison clearly shows a shift in the distribution within the classes. In 1998 65% of all vessels were in class 3, reducing to 40% in 2012. At the same time, the percentage of vessels assigned to class 4 and 5 increased from 21% and 7% up to 22% and 32%. Since 2014, a new lock has been under construction in Brunsbüttel to meet the requirements of the increasing traffic following its completion in 2021. This, however, also means that the ship-induced loads will increase with larger vessels and therefore greater effort is needed to protect the waterway. This affects both the embankments as well as the bottom of the canal requiring more dredging.

Annual dredging volumes for the western half of the Kiel Canal fairway (west of km 49.460) were provided by the local Waterways and Shipping Office (WSA Brunsbüttel, personal communication, 2016) and are available for the years 2006 to 2008 as well as for 2013 and 2014, as listed in Table 1. The numbers vary significantly from year to year in the range of a few 1×10^4 m^3/a and more than 1×10^5 m^3/a because the recorded volumes do not differentiate between annual maintenance dredging and individual measures, e.g., owing to construction. Furthermore, these numbers do not include dredging works in the Brunsbüttel locks and the lock harbors, which were of the order of 6×10^6 m^3/a to 7.6×10^6 m^3/a between 1998 and 2006 (Brockmann et al. 2008). The federal maintenance budget for the Kiel Canal ranged from 5 to 9 million Euros per year in the past 8 years (expenses set by the annual federal budget laws 2012 to 2019). These expenses explicitly exclude construction and training measures, which additionally require several million Euros each year.

Table 1: Annual dredging volumes for the Kiel Canal fairway west of km 49.460, excluding locks and lock harbors

Year	Volumen (m^3)
2006	25,954
2007	59,440
2008	65,329
2009-2012	N/A [a]
2013	109,462
2014	53,375

Source: Data from WSA Brunsbüttel, personal communication (2016).

[a] Unknown due to a lump-sum contract with a dredging company.

Data and Methods

Field Data

Field measurements took place in the cross section at canal station km 17.925 [see Fig. 2(b)] starting September 17, 2012, 10:00 a.m. (CEST) until the recovery of the measurement equipment September 25, 2012, 12:30 p.m. (CEST). In this period a total number of 509 vessels were recorded. The direction of ship traffic was found to be balanced between the locks in Brunsbüttel and Kiel. The canal was chosen for the field campaign because of its laboratory-like ambient conditions and the presence of a representative sediment grain size distribution for German coastal waterways. Owing to ship locks at both canal ends, the measurements were neither affected by tidal currents nor by naturally varying discharges. As shown in Fig. 3(d), three-dimensional (3D) flow velocities range around zero before and after the ship-induced disturbances. Considerable flows only occurred during regular dewatering periods when water was drained through the Brunsbüttel lock. Furthermore, the chosen cross section is within a straight canal section, so that maneuvering effects are also reduced to a minimum. A nearby bridge was used for a photo documentation and to set up a data logger for the Automatic Identification System (AIS) signals transmitted by passing vessels. The AIS signal provides all relevant ship and maneuvering parameters together with a timestamp, including name, identifier, geometry (such as the ship length L, the beam B or the draft T), and current position of a vessel. These parameters are referred to as AIS parameters in the following. Furthermore, traveling speed as speed over ground, draft, and direction are also broadcasted by the AIS and referred to as sailing parameters in the following (IMO 2015).

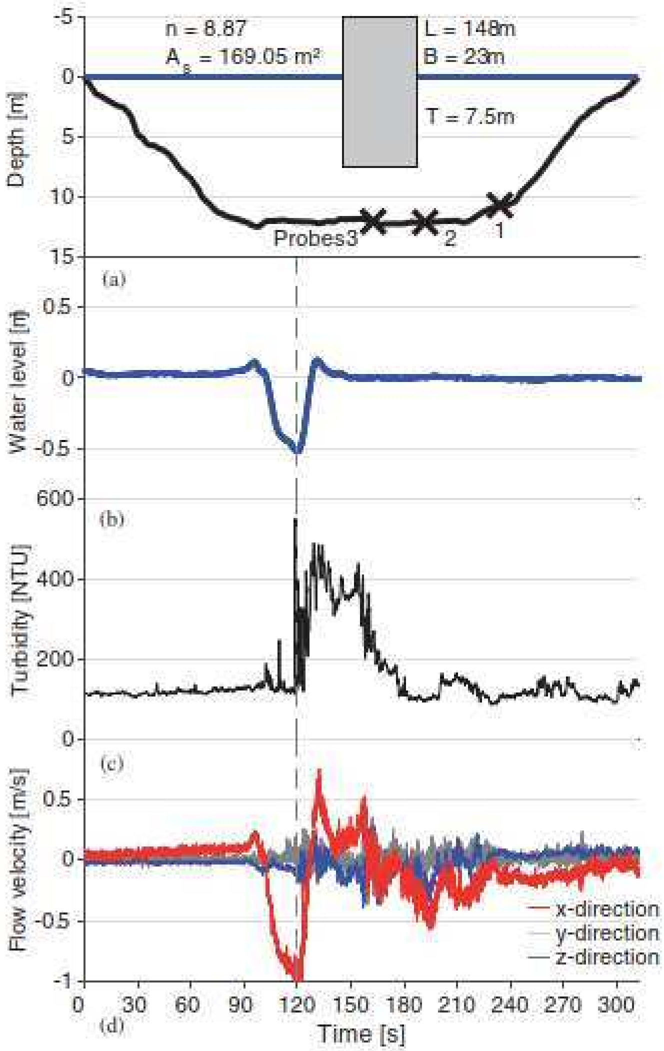

Figure 3: Overview of the recorded parameters and their development over time during a random vessel passage. From top to bottom: (a) simplified ship geometry and location of the probes; (b) water level fluctuation; (c) turbidity; and (d) flow velocity. (Adapted from Niehüser et al. 2016)

The instruments for the field campaign were located at the canal bed as sketched in Fig. 2(b). The probes are almost equally distributed in one half of the approximately symmetrical cross section: at the center of the bed (probe 3, 82.85 m), near the shore (probe 1, 43.31 m), and between the forenamed locations (probe 2, 66.61 m). All mentioned cross-channel distances refer to the southern bank of the measurement cross section.

At these three locations, conductivity (*C*), temperature (*T*), and depth (*D*) were recorded using a *CTD* profiler with a temporal resolution of 8 Hz. Depth, recorded as pressure and important for the further analysis, has an accuracy of ±0.01%, according to the manufacturer information. Turbidity of the canal water, recorded in nephelometric turbidity units (NTU), is used as surrogate variable of the suspended sediment concentration (SSC). Several water samples were taken during the measurements and evaluated in the laboratory to calibrate the conversion from turbidity to SSC. The given sediments yield a factor of 1.5 g/m^3 per NTU, which is used for conversion between SSC and NTU throughout the study whenever necessary. Turbidity was measured at 8 Hz using optical backscatter probes (Seapoint Turbidity Meter) at three locations in the canal cross section at km 17.925, as shown in Fig. 2(a). The accuracy of the measurement is specified by the manufacturer with ±2%. Together with the SSC probes, three 3D flow probes (Nortek Vector) were deployed at the canal bed. Each probe measured canal-parallel (*x* direction), cross-canal (*y* direction), and vertical (*z* direction) flow velocities at 32 Hz during the entire field campaign. The recorded flow velocities can be assumed to be representative for the entire Kiel Canal owing to the homogeneous cross section of the canal. The probes are declared with a typical error of 1% for the used measuring range of ±2 m/s. Owing to favorable conditions at the canal bed with sufficient suspended particles and no considerable air bubbles in the measuring volume, the errors are expected to be within this range specified by the manufacturer. Furthermore, a vessel-mounted acoustic Doppler current profiler (ADCP) was used to estimate the SSC distribution in the cross section during 3 days of the field campaign. The backscatter measurements were performed and evaluated by Aqua Vision BV, resulting in cross section profiles of SSC distribution of 373 individual timestamps. In addition, another optical backscatter probe was regularly lowered to the canal bed during the vessel-based measurements to record vertical turbidity profiles. The corresponding sediment grain sizes were determined using soil samples taken and analyzed also by Aqua Vision BV (Aqua Vision BV, Suspended sediment measurements in the Nord-Ostsee-Kanal, unpublished report). Owing to the homogeneous and stationary hydrodynamic conditions in the Kiel Canal, it is assumed that the measurements only deviate within the typical error ranges specified by the probe manufacturers. Furthermore, errors are assumed to be normally distributed, resulting in a constant signal noise rather than a drift over time.

The observed parameters are exemplary shown in Fig. 3 considering the passage of one individual vessel. The gray dashed line is located at time step 120 s, a relative time with respect to the starting point of the passage. This point was chosen as a common reference point for all observed passages and is defined as the point of time at which the maximum drawdown occurs. Fig. 3 also highlights the fluctuation in the water level which correlates with the recorded currents in the *x* direction. After the drawdown, the turbidity starts to increase rapidly, reaching a maximum with the stern wave peak and decreasing slowly towards its initial level.

Drawdown Estimation

Different existing empirical approaches to estimate the drawdown of a vessel in confined waters (Krey 1913; Constantine 1960; Bouwmeester et al. 1977; Gelencser 1977; Dand White 1977; Führböter et al. 1984; PIANC 1987, and the adjusted regression approach of Schoellhamer 1996) have been reviewed and used to calculate the drawdown in confined waters using the field measurement data in the Kiel Canal. The results are summarized in Fig. 7. All approaches show shortcomings in the proper description of the actual drawdown at the ship hull because they were developed for either very specific boundary conditions (e.g., Constantine 1960) or for the design of revetments focusing on the drawdown at the canal bank (e.g., Bouwmeester et al. 1977).

All methods to estimate the drawdown z_S have in common that they are subject to certain simplifications such as neglecting friction or return flow assumed being uniform. In addition, most of the existing methods are restricted to homogeneous cross-section or small cross-section ratios. Based on Bouwmeester et al. (1977), the underlying simplifications and assumptions are highlighted exemplary. Specifically, the ship speed in an approximately uniform rectangular or trapezoidal channel is assumed constant. The channel itself is straight and of infinite length. The ship hull is considered uniform, meaning that the effective shape is not taken into account. The return flow around the ship is constantly distributed over the entire cross section of the channel and the water level depression in the channel cross section owing to the passing vessel is constant along the length of the ship. Finally, the squat in the longitudinal axis of the ship is equal to the water level depression and frictional losses are not taken into account. Both the applied mass and pulse conservation laws in Bouwmeester et al. (1977) are based on these assumptions. Similarly, the approaches of Krey (1913), Constantine (1960), and Führböter et al. (1984) are based on simplifications. However, the approaches may vary due to the differences in the applied physical equations or the assumed boundary conditions. The approach of Constantine (1960), for example, is based on the continuity equation and the law of energy conservation. Führböter et al. (1984), by contrast, used the law of conservation of energy and momentum. In more empirical approaches, such as that of Gelencser (1977), model observations are combined with dimensionless factors such as the Froude number F and correction terms derived from the dataset, e.g., for the wave run-up within the determination of the drawdown z_S. An empirical-based approach relying on model experiments can be found in Dand White (1977). To adjust the Suez Canal for larger ships, three model ships were analyzed to investigate the influences of different maneuvers. Based on their measurements of water level depressions, a directly solvable approach was developed. Schoellhamer (1996) focused on the relationship between the depth-based Froude number F_h and the blocking coefficient n using dimensionless wave heights from the relationship between draft and water depth. The optimization yielded an empirical, exponential relationship based on field data. In Rapaglia et al. (2011), a field-data-based optimization also resulted in an exponential relationship of Froude number, blocking coefficient, and draft.

For the evaluation of the existing approaches, mainly large vessels were used ($n \leq 60$; $A_S \geq 31$ m^2). This reduces the analysis to vessels that potentially induce high loads and generate large water level fluctuations. Analogous to Niehüser et al. (2016), the calculation of the drawdown is based on a sample assumed being unaffected by complete measured values from all recorded ship passages. To assure that there is no influence from other passages, a time interval of 2 min before and 10 min after a ship's passage has been chosen in which no other traffic occurred. Another criteria ensures that the distance of a recorded ship passage from the nearest probe is less than 2 m. Finally, 251 ship passages were used. A total of 189 of the 251 ships have been maneuvered above probe 3 in the center of the canal, 61 vessels over probe 2, and one vessel over probe 1, located close to the southern bank.

To estimate the drawdown at the hull of a vessel without using empirical factors or exponents, a new approach was derived purely from fundamental physical equations: the law of mass conservation in the form of the continuity equation

$$A_1 \cdot v_1 = A_2 \cdot v_2 \tag{1}$$

and the law of energy conservation in the form of the Bernoulli equation

$$\frac{v_1^2}{2g} + \frac{p_1}{\rho g} + z_1 = \frac{v_2^2}{2g} + \frac{p_2}{\rho g} + z_2 \qquad (2)$$

Both laws describe the conservation for the transition between two control sections, indexed with 1 and 2, where A = the canal cross-sectional area; v = the flow velocity; p = the pressure; and z = the geodetic height component. Constants are the gravitational acceleration g and the water density ρ.

For the calculation of the drawdown z_S the two cross sections 1–1 and 2–2, as shown in Fig. 4(b), are used. Eq. (1) can be solved to v_2

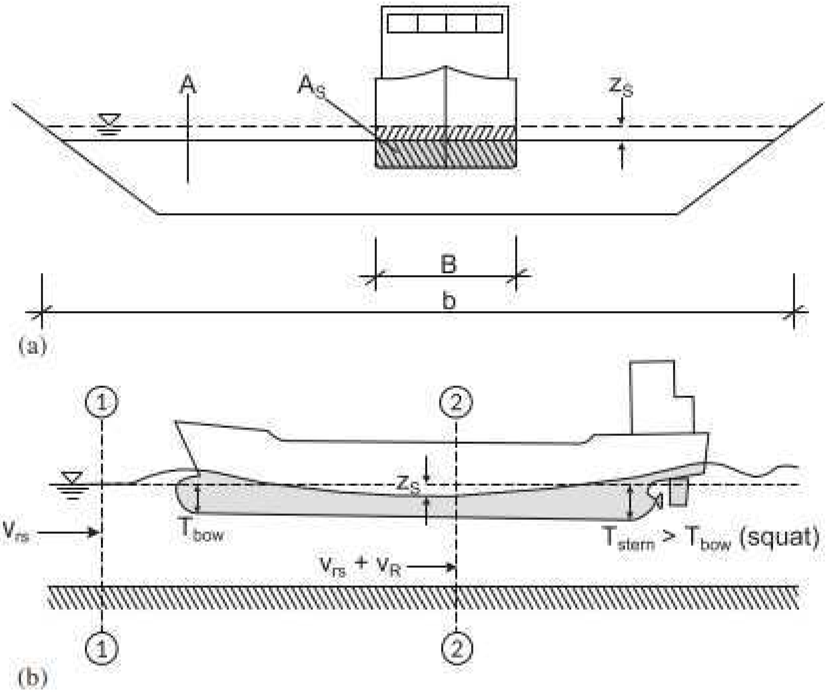

Figure 4: Considered cross section (a) and longitudinal section (b) indicating the parameters used for the development of the drawdown estimation

and rewritten as follows with reference to the given cross sections:

$$v_2 = \frac{A_1 \cdot v_1}{A_2} \qquad (3)$$

$$(v_{rs} + v_R) = \frac{A_1 \cdot v_{rs}}{(A_1 - z_S \cdot b_1 - A_S + z_S \cdot B - s \cdot B)} \qquad (4)$$

where A_S = the cross-sectional area blocked by the vessel; b_1 = the canal width at the water surface; B = the vessel width; v_{rs} = the vessels speed relative to the water column; and v_R = the return flow velocity around the vessel. The dynamic squat effect, causing a non-uniform, stern-focused increase in the vessel's draft by s and therefore causing an increase in A_S at the far end of the vessel is neglected, because the squat could not be recorded as part of the field measurements. In Fig. 4(b), the squat is indicated as the difference in draft T between bow and stern of the ship. However, a vessel geometry-dependent correction will be applied in the following steps, accounting for errors due to model assumptions and with that also accounting implicitly for the squat effect.

The Bernoulli equation [Eq. (2)] can be reduced and rearranged since pressures p_1 and p_2 are equal in an open channel and the velocities are given as depicted in Fig. 4:

$$z_S = z_1 - z_2 = \frac{1}{2g} \cdot \left(v_2^2 - v_1^2\right) \quad (5)$$

$$z_S = \frac{1}{2g} \cdot \left[(v_{rs} + v_R)^2 - v_{rs}^2\right] \quad (6)$$

Substituting ($v_{rs} + v_R$) in Eq. (6) with Eq. (4) yields an approach to estimate the drawdown z_S solely based on easily quantifiable parameters. All required parameters are available from survey (cross-sectional area of the canal A_1, canal width at the water surface b_1) or from data transmitted by the AIS parameter of the vessels (relative vessel speed v_{rs}, vessel width B, cross-sectional area of the vessel A_S derived from draft and width):

$$z_S = \frac{1}{2g} \cdot \left[\left(\frac{A_1 \cdot v_{rs}}{(A_1 - A_S - z_S \cdot b_1 + z_S \cdot B)}\right)^2 - v_{rs}^2\right] \quad (7)$$

The strong simplifications of the chosen approach, i.e., the drawdown is assumed being constant over the entire water surface width and the squat is assumed being negligible, result in a general underestimation of the drawdown. Therefore, the approach has been modified in a second step by replacing the canal width b_1 with an as-yet unknown reduced canal width b^*_1 for which the assumption of a constant drawdown is correct. The errors in the estimation due to neglecting the squat are also covered by this approach, since the correction process does not differentiate between error origins. To allow later an application of the drawdown approach, b^*_1 has to be derived from given AIS and canal parameters for each vessel. The ratio between canal and vessel cross section n, which is a dimensionless parameter describing the canal size in relation to the vessel size, has been chosen as a proxy. Here n^* is defined as follows using water depth h to describe the reduced cross-sectional area of the canal A^*_1which can be assumed to be rectangular:

$$n^* = \frac{A_1^*}{A_S} = \frac{b_1^* \cdot h}{A_S} \quad (8)$$

Different AIS parameter and parameter combinations were finally tested using correlation analyses to describe n^*. Largest correlations were found using the ratio between water depth and vessel draft h/T for the description of n^*. A linear relationship with a 95% confidence interval was derived:

$$n^* = 7 \cdot \frac{h}{T} - 5.4[\pm 1.7] \qquad (9)$$

Using Eq. (9), n^* can be estimated for any vessel. Here b^*_1 can be calculated subsequently [cf. Eq. (8)]. Substituting b_1 with b^*_1 in Eq. (7) yields the final drawdown estimation approach, which is further applied to the observational data:

$$z_S = \frac{1}{2g} \cdot \left[\left(\frac{b_1^* \cdot h \cdot v_{rs}}{(b_1^* \cdot h - A_S - z_S \cdot b_1^* + z_S \cdot B)} \right)^2 - v_{rs}^2 \right] \qquad (10)$$

Transport Estimation

The main scope of the developed sediment transport estimation approach is the comparison of (i) transported sediment volume in a canal with frequent vessel traffic with (ii) the transported volume in case that there is no traffic in the same canal. The difference of the scenarios (i) and (ii) describes the ship-induced change in sediment transport whereas the residual volume is due to natural transport processes. Applied to the recorded time series, the approach does not yield results for individual vessels but rather for the general traffic, which is more interesting and helpful from a management perspective. The estimation approach is divided into three steps: 2D turbidity approximation, transport estimation based on field data, and transport estimation based on adjusted data.

A 2D turbidity approximation is needed to extrapolate from the three point-wise turbidity measurements at the canal bed to a turbidity distribution in the canal cross section. A computational grid with quadratic cells with edge lengths of 1 m was chosen to discretize the cross section, as shown in Fig. 6(a). At the three cells where the probes are located the recorded turbidity time series are used as boundary conditions. Necessary assumptions to extrapolate the turbidity from these cells were made by using the vessel-based recorded SSC distributions as reference. The SSC distributions, based on ADCP measurements by Aqua Vision BV (Aqua Vision BV, Suspended sediment measurements in the Nord-Ostsee-Kanal, unpublished report), show the most important distribution defining patterns: during periods with no ship-induced disturbance the SSC at the water surface is approximately at two-thirds of the bed SSC. Furthermore, the surface SSC does not change significantly during periods with disturbance. Therefore, as a first step, a base turbidity bed. Signal noise was smoothed using a moving-average low-pass filter and the maximum base turbidity was defined as median of the local minimal turning points in the smoothed signal. This method allows a robust estimation of the upper limit of the base turbidity using the entire time series, because outliers and temporary turbidity increases during ship passages are ignored by the median. The maximum base turbidity was calculated as 64 NTU and was used to create a base turbidity time series by truncating all values in the smoothed signal above the maximum base turbidity (see Fig. 5).

The resulting time series was multiplied by two-thirds as a boundary condition for the surface cells in the computational grid. As a fourth sampling point at the canal bed, in addition to the three probes, the turbidity under the ship's keel is linearly interpolated using the adjacent probes. A quadratic function is finally fitted to the sampling points and turbidity values for each bed cell are computed using this function. An inverse distance weighting of the bed cells yields a similar distribution as observed with maximum turbidity under the keel and a quick lateral decrease in turbidity. The turbidity of the cells between surface and bed was finally computed by linear interpolation between the assumed surface turbidity and the calculated bed turbidity. The assumption of an almost-linear turbidity change between bed and surface was confirmed by the vertical turbidity profiles. This 2D turbidity approximation approach was applied to each time step of the 8 Hz time series. This approximation is highlighted in Fig. 6(b) whereas Fig. 6(c) shows the measured SSC distribution for the same point of time. The approach was subsequently validated using SSC distributions, which were not used for the calibration exercise.

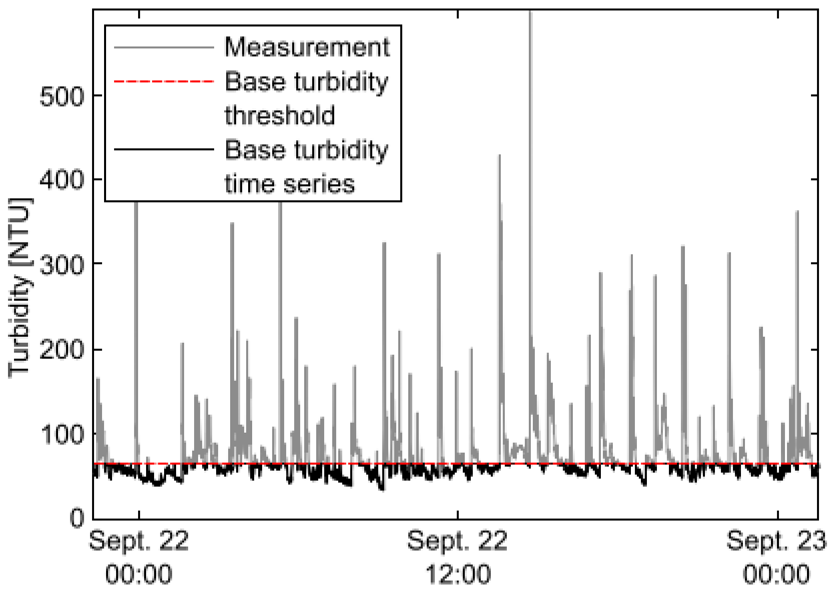

Figure 5: Base turbidity within an exemplary 24 h measurement cut-out

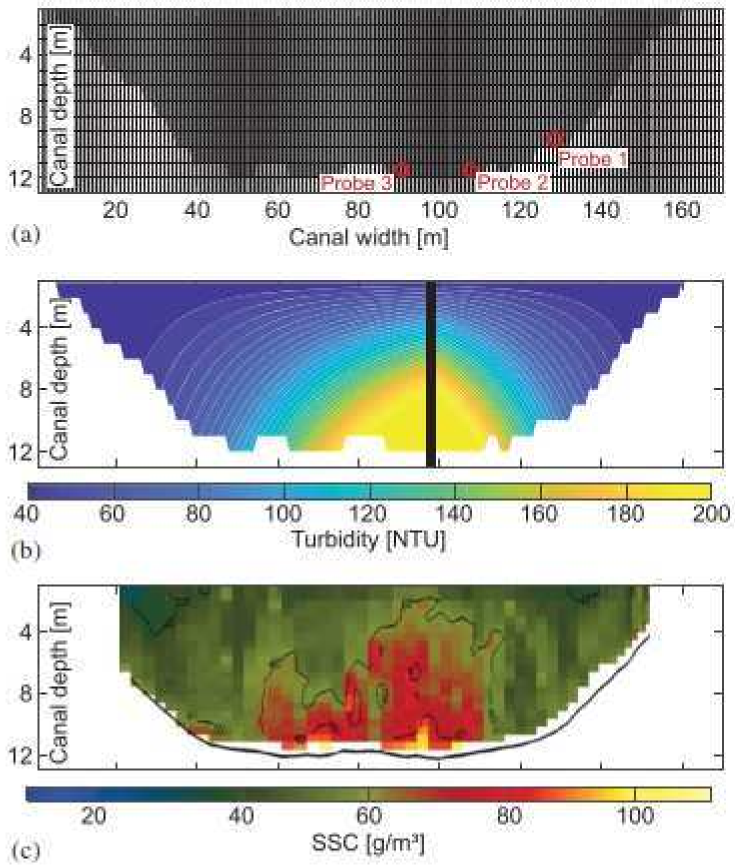

Figure 6: Grid for turbidity extrapolation (a), example turbidity extrapolation performed on the grid for a specific time step (b), and corresponding ADCP field measurement at the same time step (c)

In the next step, the approximated distributions for each time step are applied to the transport estimation. Measured flow velocities are used to estimate the transport of suspended matter along the canal axis. Prior to this, preinvestigations were conducted to determine the relevant components of the 3D flow data. An Eulerian specification of the flow field during vessel passages reveals, that canal-parallel (*x* direction) flows highly dominate the resulting flow direction whereas cross-canal (*y* direction) and vertical velocities (*z* direction) can be neglected. Therefore, only flows in the *x* direction are used for the transport estimation. Furthermore, the measured velocities at the canal bed are assumed to be representative for the entire canal cross section because there were no more detailed measurements for the water column during the current field campaign. However, Plate Keil (1971) show that this assumption is reasonable in terms of the vertically uniform distribution using vertical flow profiles from the Kiel Canal during vessel traffic. The 32 Hz *x* direction flow data are downsampled using a moving average filter to meet the 8 Hz turbidity sampling rate. For each timestep t the sediment transport rate Φ_{SSC} in g/(m$^2 \cdot$ s) is finally computed by combining the sediment concentration β_{SSC} in g/m^3 and canal-parallel flow velocity v_x in m/s:

$$\Phi_{SSC}(t) = \beta_{SSC}(t) \cdot v_x(t) \qquad (11)$$

where values of Φ_{SSC} may be positive or negative, depending on the sign of v_x. Owing to the alignment of the flow probes with the canal axis, positive *x* flows are defined as flows towards the lock at the Brunsbüttel canal end. Subsequently transport rates are directed and sediment fluxes can be interpreted directly.

In a last step, the previously conducted transport estimation is repeated with adjusted flow and SSC data to assess the ship-induced sediment transport. While the already conducted estimation yields transport rates as occurred, the estimation with adjusted data should describe the sediment transport as if there were no vessel traffic during the field campaign. Therefore, ambient conditions are derived from the measurements and used in Eq. (11). Ambient turbidity conditions are already derived from the turbidity measurements for the first step and are reused at this point. The ambient flow conditions are derived from the canal-parallel flow velocities using a moving average filter with a 60 m moving window. This filter configuration was tested against other window sizes and finally chosen because it successfully removes temporary changes in flow velocity, i.e., owing to passing vessels, but still retains velocity changes on a hourly scale which occur due the periodic canal dewatering. The averaged flow time series is then used in the transport estimation together with the ambient SSC conditions.

Results and Discussion

Drawdown Estimation and Approach Adjustment

The measurements at the cross section in the Kiel Canal show maximum water level depressions up to z_S = 1.01 m and minimum values of z_S = 0.07 m. For the comparison between the measurements of the drawdown z_S and the values calculated with the empirical formulas each set of computed drawdown data is shown as a kernel density function in Fig. 7(a). Furthermore, the residuals between the measurements and the calculated values are shown as error bars in Fig. 7(b) with the mean plotted as dots and the standard deviation as a solid line representing the symmetric distance above and below the mean. The differences in the spread are shown by the kernel densities of the different empirical approaches. The observed values of z_S are scattered widely, which is shown by the flat density function whereas the kernel densities of the empirical formulas are compressed with significantly higher peaks in the frequencies compared with the observations. The peaks of the calculated drawdown also show an offset to the left illustrating that the empirical formulas underestimate the observations. This is confirmed by the mean residuals that show differences in the magnitude of 14 to 25 cm except of the regression approach of Schoellhamer (1996). In the latter case, the mean residual of zero is reasonable because the observed values of the drawdown z_S have been used to fit the regression coefficients of the depth-based Froude number F_h and the blocking coefficient *n*. The standard deviation ranges between 8 cm regarding Bouwmeester et al. (1977) and 22 cm regarding PIANC (1987). Bouwmeester et al. (1977) also exhibited the lowest mean residual. In general, the empirical approaches based on applied physical laws (e.g., Bouwmeester et al. 1977) produce better results regarding the mean and the spread than analytical (e.g., Gelencser 1977) or diagram-based (e.g., PIANC 1987) approaches. In particular, diagram-based approaches tend to weight the individual input

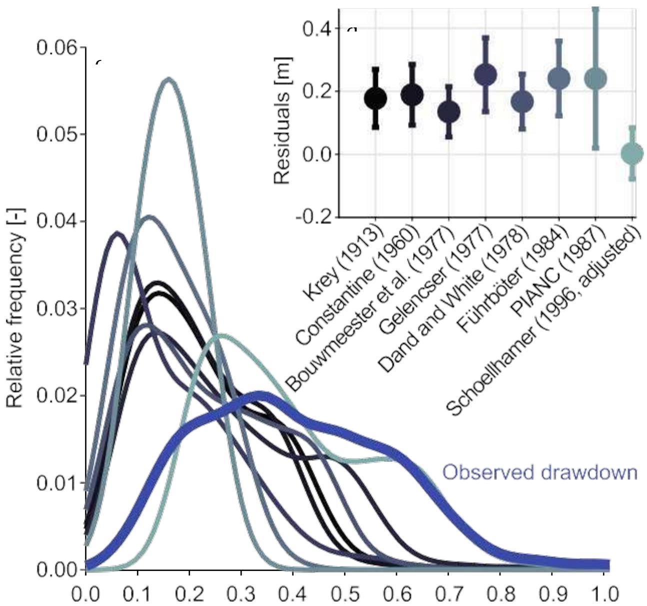

Figure 7: Calculation of the drawdown based on existing empirical approaches using the data of the field measurements in the Kiel Canal: (a) normal kernel functions for the individual approaches; and (b) the mean residuals (dots) and the corresponding standard deviation

parameter higher than others. Accordingly, when determining these approaches, it depends especially on the intended use and the available data sets (e.g., individual vessel types or model specification). For all analyzed approaches, it is difficult to quantify and discuss exactly to which parameters the residuals can be attributed. Considering the age of the approaches beginning with Krey (1913) in the early 20th century and ending in late 1980s, it should be taken into account whether the findings obtained from the comparison of the empirical approaches are due, for example, to changes in the ship geometry over the past decades (see "Study Area"). With regard to the ship size, there is a direct association with an increase of the drawdown z_S and this would explain the underestimation of the observed values because actual vessel sizes were not considered in the derivation of the approaches at that time. It is likely that the main differences in the residuals presented in this study between the empirical approaches and the observed drawdown z_S are related to this fact. Furthermore, scale effects in physical models can distort the achieved results. The specific characteristics of the Kiel Canal can also cause discrepancies in the comparison. For example, in the Kiel Canal the speed over ground is limited by law. In case that the speed over ground is highly weighted in an empirical approach, it is reasonable that differences occur. Overall, the relative influence of the required parameters in the approaches plays an important role if a dependency to the drawdown z_S is assumed which is not provided by the field measurements presented here.

As all of the approaches are based on limited data and limiting assumptions, a development of a more robust analytical approach has been conducted also to adapt for larger vessels. The aim of the development and the following optimization was to avoid unsteady correction functions by using fundamental physical equations and by improving the basic assumptions of the approach. Taking a reduced canal width b^*_1 into account, the flow around a vessel is more accurately reflected in the approach. The reduced canal width is determined by the relationship between the reduced cross-sectional ratio

n^*, water depth, and draft. A further correction of the results can be omitted due to this optimization. The application of this approach to the passages in the Kiel Canal shows that the drawdown can be estimated based on openly available data, i.e., AIS-based parameters and water levels. This allows an application of the approach to remotely collected data, e.g., with a temporary AIS antenna or to data provided via online services. Nevertheless, a verification of estimation results using direct measurements is still necessary, especially after applying the approach on a new canal geometry.

The developed approach to estimate the drawdown at the hull of a vessel [Eq. (10)] has been applied to the measured data of the Kiel Canal field campaign. Using AIS vessel data and the known waterway parameters, the drawdown has been estimated for each vessel, that passed over one of the three probes. The estimation results are compared with the measured water level depression and plotted against each others, as shown in Fig. 8(a). In Fig. 8(b) the performance of the approach compared with the empirical approaches is shown analogous to Fig. 7. The residuals between the measurements and the calculated values are plotted as error bars with the mean plotted as dots and the standard deviation as a solid line. The mean of 5.6 cm is significantly lower than the mean of the seven empirical approaches. The improvement can be assigned to the purely physics-based approach with as few assumptions as possible. Nevertheless, the simplification of the complex processes results in the remaining error that could be reduced using further measurements. Only the regression approach of Schoellhamer (1996) shows a smaller mean error, because this approach is explicitly adapted to the Kiel Canal measurements and is therefore not transferable to other waterways. The remaining, visible spread in Fig. 8(a), expressed as standard deviation in Fig. 8(b), originates from measuring uncertainties as well as local processes (e.g., wind waves) not covered by the analytical approach. However, the main goal, improving the overall description of the drawdown compared with the reviewed approaches, was achieved.

In terms of ship traffic management, empirical approaches for the estimation of the drawdown yield a practical use in engineering. Analyses of field measurements or model experiments benefit from the simplicity of the physical fundamentals, in the form of conservation laws, and can be flexibly adapted to the problems at hand. Through the analytical adaptation of the theoretical bases of observation to the measurement results, optimizations are possible to an extent that allows further practice-oriented application and can be incorporated into rules and technical regulations for the design of embankments for waterways.

Transport Estimation

Both transport estimation runs, with conditions as recorded and with ambient conditions, revealed a traffic-induced net sediment transport towards the lock at Brunsbüttel. Fig. 9(a) shows the estimated sediment transport in metric tons for both runs. Starting at 0, signed values of Φ_{SSC} for each time step were accumulated and plotted against time for the duration of the field campaign. The upper solid line indicates the transport estimation for conditions as recorded (with ships) whereas the lower solid line indicates the transport estimation for ambient conditions (without ships). Overall, both lines show a positive trend, but the development of the cumulative sediment transport over time follows a step-wise increase. Four strong increases (“steps”) can be found during the field campaign and are highlighted with dotted lines in Fig. 9(a). These steps match with periods of increased

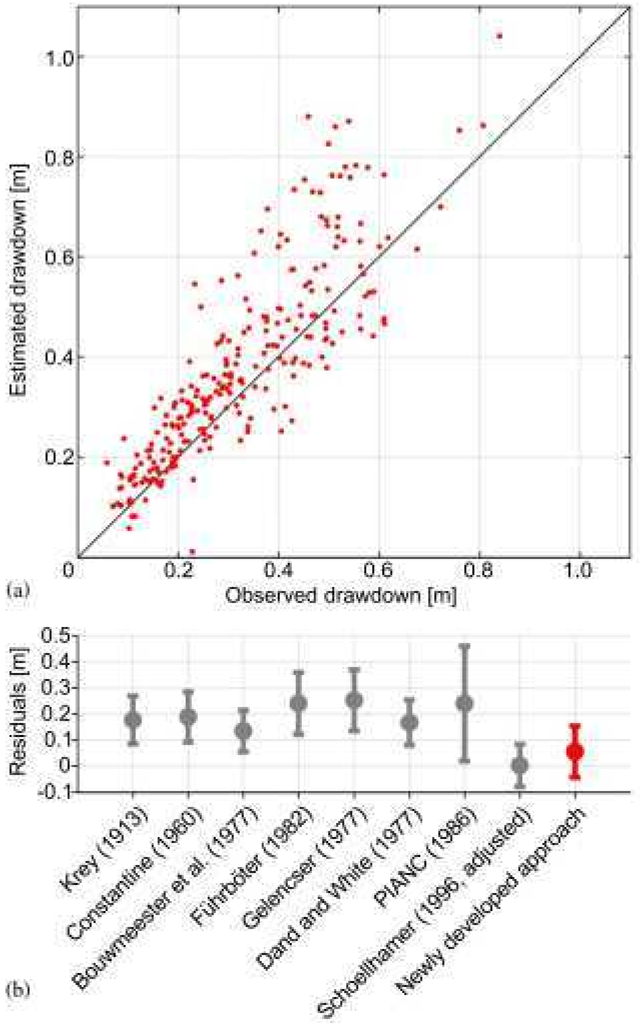

Figure 8: (a) Observed drawdown versus estimated drawdown using the newly developed approach; and (b) the performance of the approach compared with the existing empirical approaches, analogous to Fig. 7

ambient flow conditions and can be linked to four dewatering events that took place during the measurements. In Fig. 9(b) these events are visible as periods where ambient flow velocities reach up to 0.15 m/s for a few hours. During times of no dewatering, flow velocities are around zero and noisy disturbances only arise from local and short-lasting effects such as wind gusts, because the locks of the Kiel Canal prevent tidal currents or naturally varying discharges. Between the dewatering events both estimations slightly drift apart resulting in an approximately 10% lower accumulated sediment mass for the run with the data reduced by the ship traffic. This proportion of about 10% of the entirely transported sediment can be attributed to ship-induced resuspension.

The annual dredging volumes listed in Table 1 were used to validate our estimates. Therefore, the resulting transport of 580 tons during 8 days with 509 vessel passages has to be extrapolated to meet

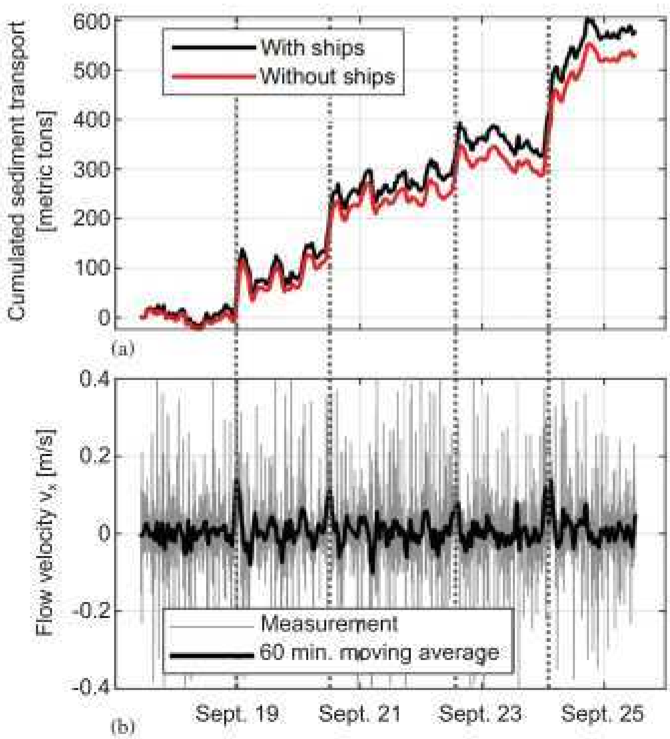

Figure 9: Transport estimation results for the entire traffic between September 17 and 25, 2012: (a) transported sediment mass, cumulated over time; and (b) flow velocity in the x direction. Dewatering periods are highlighted as dotted lines

the number of approximately 35,000 vessels that used the canal in 2012. The resulting mass of 39,695 tons is then converted to a transported sediment volume using an average sediment density of 1.857 tons/m^3. The average density is calculated from the grain size distribution determined by Aqua Vision BV based on sediment samples, and densities for each grain fraction which were estimated, e.g., by Eiffert et al. (2013), who evaluated soil parameters to estimate critical shear stresses for a nearby cross section of the Kiel Canal (km 26.020). The estimation of the totally transported sediment volume in 2012 amounts to 21,376 m^3. Comparing this estimate with the actual dredging volumes in Table 1 has to be done carefully, because the actual volumes are from the entire western Kiel Canal whereas the estimate only considers the transport through a specific cross section. Nevertheless, the estimate is in the same order of magnitude as the actual volumes.

This result gives an insight in the complex sediment transport processes because it quantifies the ship-induced amount of transported sediments for the first time. Regarding future management strategies, this estimation demonstrates that only a rather small part of the dredging can be affected, e.g., by traffic restrictions such as lower speed limits, for example as Rapaglia et al. (2015) proposed for the Venice Lagoon.

Conclusions

In the presented paper, we have described newly derived drawdown and sediment transport estimation approaches based on field measurements in the Kiel Canal, Germany.

The analytical approach to estimate the drawdown was based on fundamental physical laws. Therefore, it should be transferable to any confined waterway. As another advantage, the application only requires openly available data. Future research should, on the one hand, focus on the application of the developed drawdown estimation approaches to different datasets from other field measurements to cover a wide range of boundary conditions and vessel geometries. On the other hand, a better understanding of the wave transformation from the ship to the shore is necessary to use our drawdown estimations as input for revetment dimensioning.

The main finding of the developed engineering approach for estimating ship-induced sediment transport is that ship-induced sediment resuspension combined with even small flow rates yields a significant sediment transport in the laboratory-like Kiel Canal. The ship-induced proportion of the entirely transported mass was of the order of 10%, meaning, in return, that the by-far largest part is not transported due to vessel-related currents but rather due to ambient conditions. In the artificial Kiel Canal these ambient condition are mainly driven by dewatering currents. As there are no more detailed dredging volumes or transport masses available, there was no possibility to calibrate the estimation. However, the presented approach is solely based on field measurements in the Kiel Canal to minimize uncertainties owing to assumptions. The presented estimation of the impact of ship traffic on the local sediment regime is based on an extensive calibration of the NTU measurements against water samples of the considered cross section in the Kiel Canal. As also shown for example by Göransson et al. (2014), the NTU measurements can be used as a proxy for the complex process of sediment resuspension because this process directly affects the turbidity in the water column. In the first place, the conducted sediment transport estimation is limited to the examined cross section. However, the uniformity of the Kiel Canal allows the transfer of the results to other sections of the waterway. The approach allows a first estimation of the impact of ship traffic on the local sediment regime and a rough estimate of the ship-induced proportion of the entirely transported sediment mass. This meets the main objective of the research cooperation by providing authorities and decision-makers a better understanding of the interaction between vessel and waterway. Future design or management decisions can be based on this understanding. This may include traffic restrictions, a widening and/or deepening of the canal, or improved revetment design. Furthermore, the knowledge gained about the sediment transport processes can be used to improve the dredging schedule. As a next step, the developed sediment transport estimation approach should be applied to different waterways to improve the understanding of the effect of ambient conditions on the totally transported sediment mass. Tidal rivers, such as the Elbe estuary, have to cope with large amounts of sediment, which are transported upstream owing to tidal currents. The quantification of the ship-induced proportion can help to improve the waterway management, similar to the management decision support for the Kiel Canal, provided with the presented study.

Data Availability Statement

Some or all data, models, or code generated or used during the study are available from the corresponding author by request. Available are: field measurement data, unpublished measuring reports, and scripts used for the presented analyses.

References

Bezuijen, A., and H.-J. Köhler. 1996. “Filter and revetment design of water imposed embankments induced by wave and draw-down loadings.” Geosynthetics: Applications, Design and Construction, edited by M. B. De Groot, G. Den Hoedt, and R. J. Termaat, 1007–1023. Rotterdam, Netherlands: Balkema.

Bouwmeester, J., E. J. van de Kaa, H. A. Nuhoff, and R. G. J. van Orden. 1977. Recent studies on push-towing as a base for dimensioning waterways. Rep. No. 194. Delft, Netherlands: Delft Hydraulics Laboratory.

Brockmann, J., A. Heeling, M. Pohl, and K. Uliczka. 2008. “The Kiel Canal.” In Vol. 74 of Die Küste, 317–332. Heide, Holstein, Germany: Boyens.

Constantine, T. 1960. “On the movement of ships in restricted waterways.” J. Fluid Mech. 9 (2): 247–256. https://doi.org/10.1017/S0022112060001080.

Dam, K. T., K. Tanimoto, and E. Fatimah. 2008. “Investigation of ship waves in a narrow channel.” J. Mar. Sci. Technol. 13 (3): 223–230. https://doi.org/10.1007/s00773-008-0005-6.

Dand, I. W., and W. R. White. 1977. “Design of navigation canals.” In Symp. on Aspects of Navigability of Constraint Waterways including Harbour Entrances, Delft, The Netherlands.

Eiffert, F., O. Niekamp, and S. Meesenburg. 2013. “Schiffsbedingte Erosion am Nord-Ostsee-Kanal [Ship-induced erosion in the Kiel Canal].” [In German.] HANSA Int. Marit. J. 150 (9): 116–119.

Flügge, G., and K. Uliczka. 1996. “Schiffsbedingte Wellen unter den spezifischen Randbedingungen von Seewasserstraßen [Ship waves under the specific boundary conditions of coastal waterways].” [In German.] In Vol. 9 of Dresdner Wasserbauliche Mitteilungen, 75–90. Dresden, Germany: TU Dresden.

Führböter, A., H.-H. Dette, and J. Jensen. 1984. Untersuchungen über schiffserzeugte Wellen an der Unterelbe in den Jahren 1980/81 [Investigations on ship waves on the Lower Elbe in 1980/81]. [In German.] Rep. No. 546. Braunschweig, Germany: Leichtweiß-Institut für Wasserbau, TU Braunschweig.

Gelencser, G. J. 1977. “Drawdown surge and slope protection, experimental results.” In Proc., 24th Int. Navigation Congress, 21–40. Leningrad, Russia: Permanent International Association for the Navigation Congresses.

Gelinas, M., H. Bokuniewicz, J. P. Rapaglia, and K. M. M. Lwiza. 2013. “Sediment resuspension by ship wakes in the Venice lagoon.” J. Coastal Res. 29 (1): 8–17. https://doi.org/10.2112/JCOASTRES-D-11-00213.1.

Gharbi, S., G. Valkov, S. Hamdi, and I. Nistor. 2010. “Numerical and field study of ship-induced waves along the St. Lawrence Waterway, Canada.” Nat. Hazards 54 (3): 605–621. https://doi.org/10.1007/s11069-009-9489-6.

Göransson, G., M. Larson, and J. Althage. 2014. “Ship-generated waves and induced turbidity in the Göta Älv river in Sweden.” J. Waterw. Port Coastal Ocean Eng. 140 (3): 04014004. https://doi.org/10.1061/(ASCE)WW.1943-5460.0000224.

Hamill, G. A., H. T. Johnston, and D. P. Stewart. 1999. “Propeller wash scour near quay walls.” J. Waterw. Port Coastal Ocean Eng. 125 (4): 170–175. https://doi.org/10.1061/(ASCE)0733-950X(1999)125:4(170).

Houser, C. 2011. “Sediment resuspension by vessel-generated waves along the Savannah river, Georgia.” J. Waterw. Port Coastal Ocean Eng. 137 (5): 246–257. https://doi.org/10.1061/(ASCE)WW.1943-5460.0000088.

Initiative Kiel-Canal E. V. (IKC). 2013. Lebensader Nord-Ostsee-Kanal [Lifeline Kiel Canal]. [In German.] https://initiative-kiel-canal.de/wp-content/uploads/2016/10/Journal_IKC.pdf.

International Maritime Organization (IMO). 2015. Revised Guidelines for the onboard operational use of shipborne automatic identification systems (AIS). Resolution A.1106(29). London: IMO.

Jensen, J. 1998. “Ermittlung von schiffserzeugten Belastungen an Wasserstraßen [Investigation of ship-generated loads on waterways].” [In German.] Numerische Verfahren in der Wasserbaupraxis, edited by J. Jensen and A. Braxein. Siegen, Germany: FWW.

Ji, S., A. Ouahsine, H. Smaoui, and P. Sergent. 2014. “3D modeling of sediment movement by ships-generated wakes in confined shipping channel.” Int. J. Sediment Res. 29 (1): 49–58. https://doi.org/10.1016/S1001-6279(14)60021-4.

Krey, H. 1913. “Fahrt der Schiffe auf beschränktem Wasser [Ship cruise in limited waters].” [In German.] Schiffbau, 14(12–17).

Niehüser, S., M. Ulm, A. Arns, J. Jensen, V. Kelln, K. Uliczka, and B. Kondziella. 2016. “Interaction between ship-induced stress and associated characteristics of turbidity records.” In Vol. 4 of Proc., 4th MASHCON 2016. Int. Conf. on Ship Manoeuvring in Shallow and Confined Water with Special Focus on Ship Bottom Interaction, 16–26. Hamburg, Germany: Federal Waterways Engineering and Research Institute. https://doi.org/10.18451/978-3-939230-38-0_3.

Permanent International Association of Navigation Congresses (PIANC). 1987. Guidelines for the Design and Construction of Flexible Revetments Incorporating Geotextiles for Inland Waterways. Permanent Technical Committee I – Working Group 4. Brussels, Belgium: PIANC.

Pesce, M., S. Terzi, R. I. M. Al-Jawasreha, C. Bommarito, L. Calgaro, S. Fogarin, E. Russo, A. Marcomini, and I. Linkova. 2018. "Selecting sustainable alternatives for cruise ships in Venice using multicriteria decision analysis." Sci. Total Environ. 642: 668–678. https://doi.org/10.1016/j.scitotenv.2018.05.372.

Plate, U., and G.-W. Keil. 1971. "Sediment-Transport in einem Seeschiffahrtskanal [Sediment transport in a coastal waterway]." [In German.] Die Küste 21: 59–65. https://hdl.handle.net/20.500.11970/101001.

Rapaglia, J. P., L. Zaggia, K. Parnell, and G. Lorenzetti. 2015. "Ship-wake induced sediment remobilization: Effects and proposed management strategies for the Venice Lagoon." Ocean Coastal Manage. 110:1–11. https://doi.org/10.1016/j.ocecoaman.2015.03.002.

Rapaglia, J. P., L. Zaggia, K. Ricklefs, M. Gelinas, and H. Bokuniewicz. 2011. "Characteristics of ships' depression waves and associated sedi- ment resuspension in Venice Lagoon, Italy." J. Mar. Syst. 85 (1–2): 45–56. https://doi.org/10.1016/j.jmarsys.2010.11.005.

Schoellhamer, D. H. 1996. "Anthropogenic sediment resuspension mechanisms in a shallow microtidal estuary." Estuarine Coastal Shelf Sci. 43 (5): 533–548. https://doi.org/10.1006/ecss.1996.0086.

Thormählen, C. 2010. "Modernisation of the Brunsbüttel locks." PIANC Yearbook, edited by L. van Schel, 131–134. Brussels, Belgium: PIANC.

Uliczka, K., and B. Kondziella. 2016. "Ship-Induced Sediment Transport in Coastal Waterways (SeST)." In Proc., 4th MASHCON – Int. Conf. on Ship Manoeuvring in Shallow and Confined Water with Special Focus on Ship Bottom Interaction, edited by K. Uliczka, C.-U. Böttner, M. Kastens, K. Eloot, G. Delefortrie, M. Vantorre, M. Candries, and E. Lataire. Karlsruhe, Germany: Federal Waterways Engineering and Research Institute.

Ulm, M., S. Niehüser, A. Arns, J. Jensen, B. Kondziella, and K. Uliczka. "Estimating ship-induced sediment transport in confined waters." In Vol. 19 of Proc., EGU General Assembly Conf. Abstracts, Munich, Germany: European Geosciences Union.

Weilbeer, H. 2014. "Sediment Transport and Sediment Management in the Elbe Estuary." In Vol. 81 of Die Küste, 409–426. Karlsruhe, Germany: Federal Waterways Engineering and Research Institute.

Zaggia, L., G. Lorenzetti, G. Manfé, G. M. Scarpa, E. Molinaroli, K. E. Parnell, J. P. Rapaglia, M. Gionta, and T. Soomere. 2017. "Fast shoreline erosion induced by ship wakes in a coastal lagoon: Field evidence and remote sensing analysis." PLoS One 12 (10): 1–23. https://doi.org/10.1371/journal.pone.0187210.

Authors:

Marius Ulm
University. of Siegen, Research Institute for Water and Environment
Paul-Bonatz-Str. 9-11, 57076 Siegen, NW, Germany
E-Mail: marius.ulm@uni-siegen.de

Sebastian Niehüser
University. of Siegen, Research Institute for Water and Environment
Paul-Bonatz-Str. 9-11, 57076 Siegen, NW, Germany
E-Mail: sebastian.niehueser@uni-siegen.de

Bernhard Kondziella
Federal Waterways Engineering and Research Institute (BAW)
Wedeler Landstr. 157, 22559 Hamburg, Hamburg, Germany
E-Mail: bernhard.kondziella@baw.de

Arne Arns
University. of Siegen, Research Institute for Water and Environment
Paul-Bonatz-Str. 9-11, 57076 Siegen, NW, Germany
E-Mail: arne.arns@uni-siegen.de

Jürgen Jensen
University. of Siegen, Research Institute for Water and Environment
Paul-Bonatz-Str. 9-11, 57076 Siegen, NW, Germany
E-Mail: juergen.jensen@ uni-siegen.de

Klemens Uliczka
Federal Waterways Engineering and Research Institute (BAW)
Wedeler Landstr. 157, 22559 Hamburg, Hamburg, Germany
E-Mail: klemens.uliczka@baw.de